# Final Scientific Report

## Executive summary:

The natural subsurface is highly heterogeneous with minerals distributed in different spatial patterns. Fundamental understanding of how mineral spatial distribution patterns regulate sorption process is important for predicting the transport and fate of chemicals. Existing studies about the sorption was carried out in well-mixed batch reactors or uniformly packed columns, with few data available on the effects of spatial heterogeneities. As a result, there is a lack of data and understanding on how spatial heterogeneities control sorption processes. In this project, we aim to understand and develop modeling capabilities to predict the sorption of Cr(VI), an omnipresent contaminant in natural systems due to its natural occurrence and industrial utilization. We systematically examine the role of spatial patterns of illite, a common clay, in determining the extent of transport limitation and scaling effects associated with Cr(VI) sorption capacity and kinetics using column experiments and reactive transport modeling.

Our results showed that the sorbed mass and rates can differ by an order of magnitude due to of the illite spatial heterogeneities and transport limitation. With constraints from data, we also developed the capabilities of modeling Cr(VI) in heterogeneous media. The developed model is then utilized to understand the general principles that govern the relationship between sorption and connectivity, a key measure of the spatial pattern characteristics. This correlation can be used to estimate Cr(VI) sorption characteristics in heterogeneous porous media. Insights gained here bridge gaps between laboratory and field application in hydrogeology and geochemical field, and advance predictive understanding of reactive transport processes in the natural heterogeneous subsurface. We believe that these findings will be of interest to a large number of environmental geochemists and engineers, hydrogeologists, and those interested in contaminant fate and transport, water quality and water composition, and natural attenuation processes in natural systems.

# Actual accomplishments

The project has led to two AGU presentations and one published paper in Environmental Science & Technology, with another one in preparation. We briefly summarize the accomplishment below.

Anionic Cr(VI) is highly mobile and poses significant environmental risks (Mohan and Pittman, 2006; Owlad et al., 2009; Richard and Bourg, 1991). Cr(VI) sorption on clays is important in controlling its transport and fate in natural subsurface environments (Fonseca et al., 2009; Khan et al., 2010; Lu et al., 2010). Most studies used well-mixed batch reactors and homogeneously packed columns. Large discrepancies have been documented between well-mixed batch reactors and natural subsurface (Chai et al., 2009; Fox et al., 2012; Krishna et al., 2000; Miller et al., 2010; Smith et al., 1997; Vereecken et al., 2011). The natural subsurface typically exhibits spatial variations in physical and geochemical properties at multiple scales (Jin et al., 2011; Landrot et al., 2012; Peters, 2009). The role of physical heterogeneity has been extensively studied in the past decades (Dagan, 1990; Gelhar, 1986) (Simunek and van Genuchten, 2008; Vangenuchten and Wierenga, 1976). Although the chemical heterogeneity is also important, it has not received much attention until recently (Simunek and van Genuchten, 2008; Vangenuchten and Wierenga, 1976). There is a significant lack of experimental data on Cr(VI) sorption to systematically understanding and quantifying the role of spatial distribution patterns in controlling sorption process. As a result, accurate prediction of reactive transport, natural attenuation, and remediation in heterogeneous natural subsurface is challenging. Therefore, the objective here is 1) to systematically understand how, to what extent, and under what conditions spatial heterogeneities regulate Cr(VI) sorption macrocapacity and macrokinetics at the column scale, and 2) to identify key measures of spatial patterns that control Cr(VI) sorption in heterogeneous media.

In the ES&T paper, we publish experimental observation and analysis from flow-through experiments were carried out at 0.6, 3.0 and 15.0 m/day using columns packed with the same illite and quartz mass however with different patterns and permeability contrasts. We define sorption macrocapacity as the total mass of sorbed Cr(VI) and macrorates as the rates of Cr(VI) sorption at the column-scale. We found that macrocapacity and macrorates decrease with transport connectivity, a quantitative measure of heterogeneity characteristics. At 0.6 and 3.0 m/day, well-connected low permeability illite zone oriented in the flow-parallel direction leads to diffusion-controlled mass transport limitation for accessing sorption sites. This results in up to 1.4 order of magnitude lower macrocapacity and macrorates compared to those in minimally-connected columns with uniformed distributed illite and quartz. At 15.0 m/day, effects of spatial heterogeneities are less significant (up to a factor of 2.8) owing to the close to chemical kinetics-controlled condition. The column-scale macrocapacity can reach the intrinsic microcapacity in low connectivity columns under low flow conditions where the residence time is comparable to or longer than the intrinsic sorption equilibrium time. Although the column-scale macrocapacity can reach full sorption capacity under low flow conditions, the macrorates are $10^{-1}$ to $10^{-3}$ of the microrates measured in well-mixed reactors.

The second manuscript (in preparation) extrapolate observations from experimental conditions to a wide range of conditions using two-dimensional reactive transport modeling.

The effects of permeability contrast between illite and quartz zones and transverse dispersivity $\alpha_T$ were analyzed. These two variables are essential in determining the diffusion-controlled mass transport between the illite and quartz zones, with higher values leading to higher macrocapacity. Two sets of spatial patterns with the same permeability mean but different $\sigma_{lnK}^2$ (variance of lnK) of 4.5 and 0.2 were generated using sequential gaussian simulation (SGS) at different correlation lengths and column lengths. Relative longitudinal correlation length ($\lambda_L$) and connectivity exert significant control on sorption macrocapacity and macrokinetics, especially for patterns with high $\sigma_{lnK}^2$. The role of spatial heterogeneities becomes more important as $\lambda_L$ and connectivity increases, which can lead macrocapacity and macrorates up to 1.5 orders of magnitude lower than the well mixed patterns.

## Project activities

Original hypotheses and approaches used. The original objective of the project is to examine the role of geochemical heterogeneity in determining scaling effects associated with the kinetics of Cr(VI) reduction by ferrous ion using column experiments and reactive transport modeling. The sediment was composed of quartz and illite, with the former representing the major component in coarse-grained materials at the Hanford site, and the latter representing the major component in fine-grained materials with high sorbing capacity. Fe(II) was sorbed to illite before the column experiments and the illite with absorbed Fe(II) was served as the source of Fe(II) for the reduction of Cr(VI) during the column experiments. Column experiments were carried out with different mineral distribution patterns and flow velocities. The two minerals were mixed with the same mass ratio, but packed with different spatial patterns within the column, as shown in Figure 1.

The original hypotheses were as follows:

- The spatial distribution of Fe-saturated illite has a large impact on the Cr(VI) reduction rate at the column scale. Column scale Cr(VI) reduction rate is slower in the case where Fe-saturated illite is distributed as one large layer (Case C) than in the case where it is homogeneously distributed along the column (Case A).

- Flow velocities have a large impact on the magnitude of scaling effects induced by geochemical heterogeneities because of the coupling between flow, transport, and reaction processes.

Problems encountered. The Cr(VI) reduction by Fe(II) reaction needs anaerobic condition, because Fe(II) can be easily oxidized by oxygen. The whole experiment, including absorbing Fe(II) onto illite, column packing, flow through experiment, sample collection and analysis, was carried out in an anaerobic chamber. It turned out that it was very challenging to maintain the anaerobic condition for every single step during the column experiments and that the Fe(II) was easily oxidized by oxygen. This challenge led to the shift in research direction to Cr(VI) sorption, which does not require anaerobic condition however still represent a large gap in understanding the role of spatial heterogeneities in determining chemical reactions. Cr(VI) sorption on clays is another important process for Cr(VI) attenuation and remediation in natural environments. The new hypotheses were similar to the original ones:

•The spatial distribution of illite has a large impact on the Cr(VI) sorption capacity and rate at the column scale. Column scale Cr(VI) sorption rate is slower in the case where illite is distributed as one large layer (Case C) than in the case where it is homogeneously distributed along the column (Case A).

•Flow velocities have a large impact on the magnitude of scaling effects induced by geochemical heterogeneities because of the coupling between flow, transport, and reaction processes.

**Departure from planned methodology.** In addition to the few spatial patterns proposed originally, more spatial patterns with different permeability contrasts were added, as shown in Figure 1. We also added the permeability contrast as an additional testing variable and examine two, instead of one, sets of columns with different permeability contrast. The *C* columns have illite and quartz grains with the same size range of 210-300 μm to minimize the effects of physical heterogeneity to the extent possible and to primarily focus on the effects of chemical heterogeneity. The *PC* columns have smaller illite grains (75-150 μm) compared to that of quartz (350-420 μm) and therefore to combine effects of physical and chemical heterogeneities. For comparison, Cr(VI) sorption in batch reactors were also carried out to quantify the intrinsic microcapacity and microkinetics under well-mixed conditions.
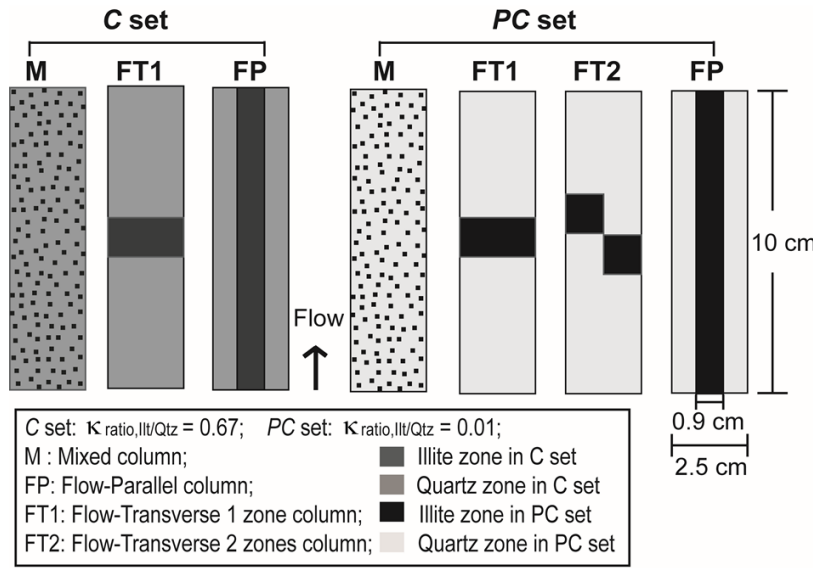


Figure 1. Two dimensional cross-sectional schematics of the 7 columns with different spatial distribution patterns of illite and quartz. The illite-over-sand permeability ratio, $\kappa_{ratio,Ilt/Qtz}$, differ in the *C* and *PC* sets. Each set has the same total mass of illite and quartz. The *C* columns have illite and quartz grains with the same size range of 210-300 μm to minimize the effects of physical heterogeneity to the extent possible and to primarily focus on the effects of chemical heterogeneity. The *PC* columns have smaller illite grains (75-150 μm) compared to that of quartz (350-420 μm) and therefore to combine effects of physical and chemical heterogeneities. Within each column set, the Mixed column (M) has illite uniformly distributed within the quartz matrix; the Flow-transverse 1 zone column (FT1) has illite in one horizontal layer in the direction perpendicular to the main flow; the Flow-parallel column (FP) has illite in one cylindrical zone in the direction parallel to the main flow. The *PC* set has an additional Flow-transverse 2 zones

4

column (FT2) where illite is horizontally distributed in 2 zones in the middle of the column, with one zone in the upper left and the other in the lower right.

Transport Connectivity ($CT_{95\%}$) (Knudby and Carrera, 2005) was used as a quantitative measure for spatial heterogeneities as well as for sorption capacity and kinetics. It compares the time for 95% arrival to the average residence time as shown below:

$$CT_{95\%} = \frac{t_{95\%}}{\tau}$$

Where $t_{95\%}$ is the time when the effluent bromide reaches 95% of the inlet concentration (s), and $\tau$ is the residence time calculated as the total pore volume of the column divided by the overall flow rates (s).

**Impacts of the project results: Effects of Spatial Patterns and Permeability Contrasts at different flow conditions**

The Cr(VI) breakthrough curves and sorbed chromium evolution for all patterns are shown in Figure 2. The addition of illite spatial patterns with different permeability contrasts confirmed our hyphotheses that illite spatial patterns exert significant control on Cr(VI) sorption capacity and kinetics, expecially at low flow velocity conditions.

At 0.6 m/day, Cr(VI) breaks through much earlier from the *PC* columns than from the *C* columns. FP PC has the earliest breakthrough, the least sorbed Cr(VI) and the lowest rate. The macrocapacity $C_{sc,m}$ for all *C* columns are similar, but different for *PC* columns. The FT1 data almost overlaps with the M column and are not shown here. At 3.0 m/day, the Cr(VI) breakthrough curves and sorbed chromium evolution are similar to those at 0.6 m/day for all columns. At 15.0 m/day, however, the macrocapacity for all columns are much lower. At 15.0 m/day, the residence time of 3.9 min is much shorter than the 20 min that is needed to access most of the external sites. The difference across columns within each set is much smaller, indicating the less significant role of spatial heterogeneities under high flow conditions.

The fact that FT1 and M are similar and are different from the FP columns indicates the importance of the zonation orientation relative to the main flow direction. In FT1, the Cr(VI)-containing inlet solution can flow through the low permeability illite zone and therefore all surface sites are accessible. In FT2 and FP PC, sorption sites can only be accessed through diffusion, with the diffusion length much longer than grain scale. To access all sites, more time are needed than residence time (98 min). Only small amount of the surface sites are accessible for FT2 and FP PC.
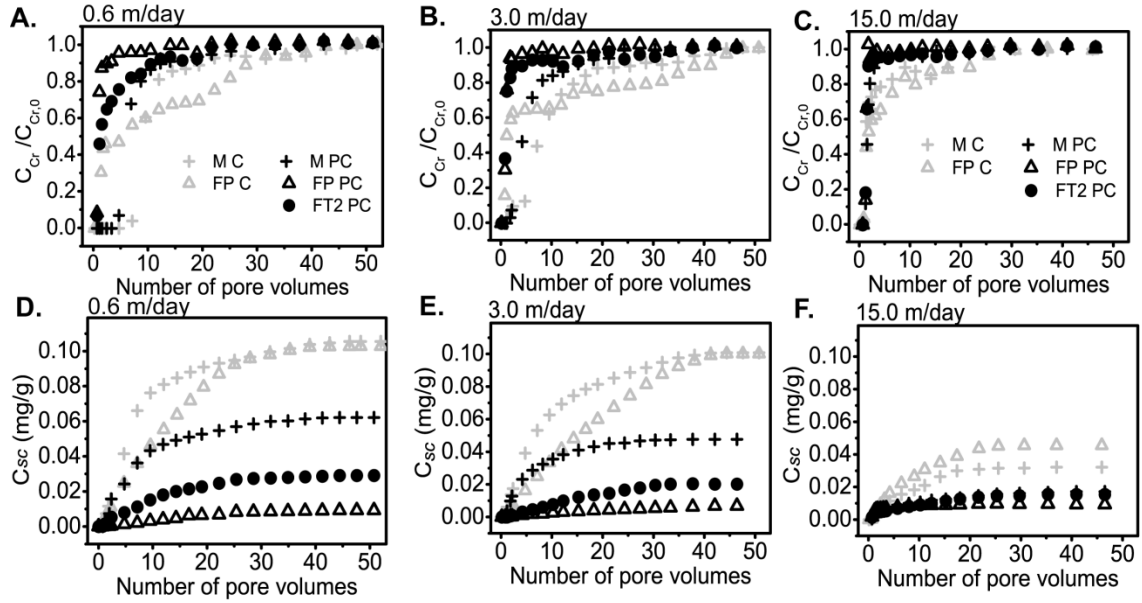
Figure 2. Evolving Cr(VI) effluent normalized concentrations (top) and cumulative sorption mass (bottom) at 0.6 (left), 3.0 (middle) and 15.0 m/day (right) for the C (gray) and PC columns (black). The residence times are 98.13, 19.63 and 3.93 minutes, respectively. The FT1 data are not shown here because it almost overlaps with the M column. Note that the total illite surface area was 144 $m^2$ in the *C* columns, almost 2 times that of the 81 $m^2$ in the *PC* columns.

**Connectivity Controls**

Our second objective is to identify key measures of spatial patterns that control Cr(VI) sorption in heterogeneous media. We found that, connectivity, a quantitative measure of heterogeneity characteristics, exerts a significant control on sorption macrocapacity and macrokinetics, especially at low flow velocities relevant to groundwater. The summary results are shown in Figure 3.

Sorption macrocapacity and macrokinetics decrease with connectivity. All macrokinetic rates are lower than the microkinetic rates. At 15.0 m/day, macrorates are highest and close to chemical kinetic-controlled regime. Macrocapacity values are the same as the microcapacity ($\gamma_c=1$) only in low connectivity columns at 0.6 and 3.0 m/day. The $\gamma_{k1}$ and $\gamma_{k2}$ decrease with increasing connectivity due to diffusion-controlled mass transport limitation imposed by the low permeability illite zone. The deviation of $\beta$ values from 1.0, increases with increasing connectivity, with the FP PC having the largest deviation. At 15.0 m/day, the deviation from 1.0 is much smaller.

The data here indicates that chemical heterogeneity alone causes much less effects than the coupled chemical and physical heterogeneities. Among the three C columns, although illite spatial patterns are the same as the PC columns, the capacity and rates are very similar. Only in PC columns where the illite permeability is 2 orders of magnitude lower than that of quartz, the effects of spatial patterns are significant. The general trend of macrokinetic rates increasing with increasing velocity and decreasing connectivity confirms conclusions from earlier stochastic analyses on single sorbing solutes (Espinoza and Valocchi, 1997; MirallesWilhelm and Gelhar, 1996). These analyses show that the time scale of sorption, which is inverse of

sorption rates, increases with correlation length (positively correlates to connectivity) and decreases with flow velocity (Deng et al., 2014; Setshedi et al., 2014).
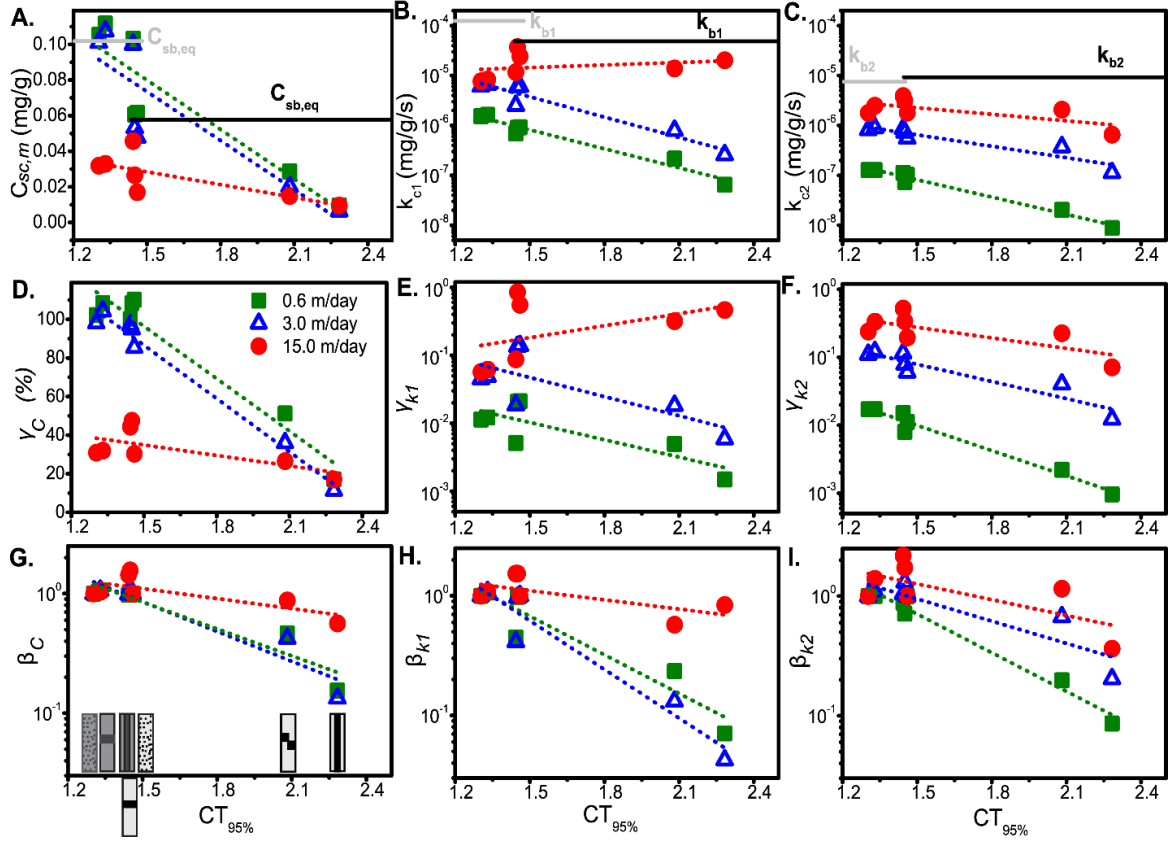


Figure 3. Cr(VI) sorption parameters as a function of the transport connectivity (CT$_{95\%}$) under different flow conditions. (A) total sorbed mass C$_{sc,m}$, (B) early sorption rate k$_{c1}$, and (C) late sorption rate k$_{c2}$. For comparison the two microkinetic rate constants k$_{b1}$ and k$_{b2}$ are also shown here for *C* (gray) and *PC* (black) as horizontal lines. (D) – (F): $\gamma$ values comparing macro- to microvalues. Macrocapacities are within an order of magnitude lower than the microcapacities; macrorates are 1 to 3 orders of magnitude lower than the microrates. (G) – (I): $\beta$ values comparing zonation columns to their corresponding Mixed columns. The impacts of spatial heterogeneities are within a factor of 2.0 under high flow condition (15 m/day) and can reach close to 2 orders of magnitude under low flow conditions (0.6 and 3.0 m/day). The dashed lines here are to help visually connect the symbols of the same flow condition however they do not necessarily suggest linear relationship between the variables.

**Reactive transport modeling in heterogeneous porous media.**

The 2D reactive transport modeling with experiment conditions was used to reproduce the experimental data, as shown in Figure 4. The simulated Br and Cr(VI) breakthrough curves (BTCs) can reproduce the data well for all columns. And the modeling parameters such as $\alpha_L$, $\alpha_T$ and surface site density were obtained. The parameters obtained from matching the experimental data were used to simulate more columns with different permeability contrasts, correlation lengths and column lengths.
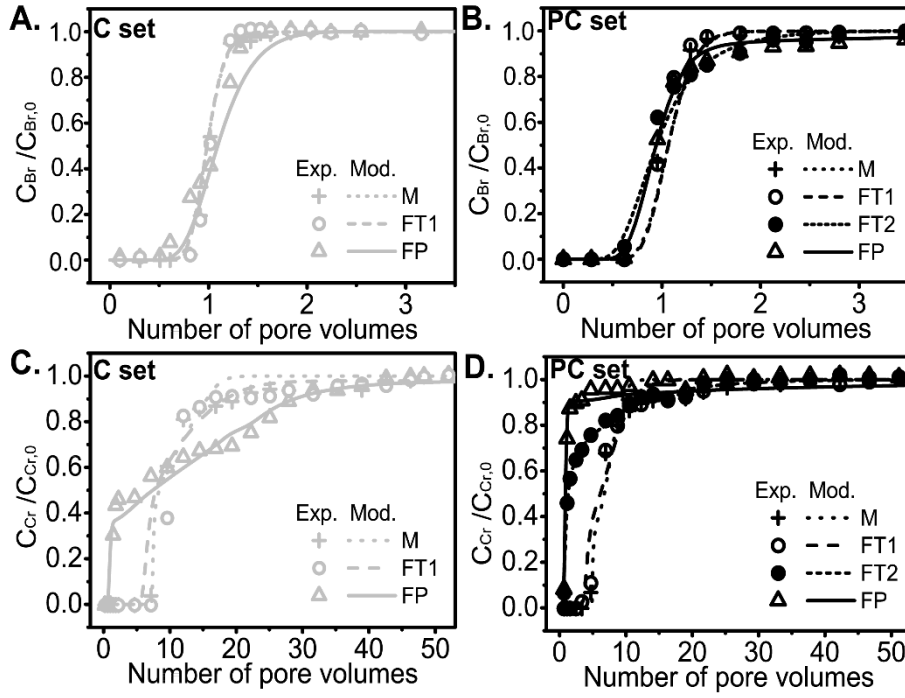
Figure 4. Experimental Br (A and B) and Cr(VI) (C and D) breakthrough data (symbols) and modeling output (lines) for the *C* columns (gray) and *PC* columns (black). The flow velocity is 0.6 m/day with a residence time of 98.13 min.

More spatial patterns that were similar to the natural subsurface (Deutsch CV, 1992) were generated at permeability variances (σ2lnK) of 4.5 and 0.2. The effects of column lengths, permeability variances, correlation lengths and connectivity on sorption capacity and kinetics were examined, as shown in Figure 6. The $\beta c$ value compares the sorption capacity between zonation columns and their corresponding Mixed columns. Large deviation of $\beta c$ values from one means large differences between zonation and mixed columns and therefore indicates the significance of spatial heterogeneities.

All $\beta_C$ values increase with increasing column length, and are close to one when column length is longer than 40 and 80 cm for $\sigma^2_{lnK}$ of 4.5 and 0.2, respectively. That means the effects of spatial heterogeneities become less significant as the length scale increases. All $\beta_C$ values decrease with increasing $\lambda_L$ (correlation length/column length) and connectivity ($CT_{95\%}$), which indicates that the effects of spatial heterogeneities are more significant in determining sorption capacity and kinetics when the reactive zones are relative large compare to the whole domain or when the domain is well-connected.
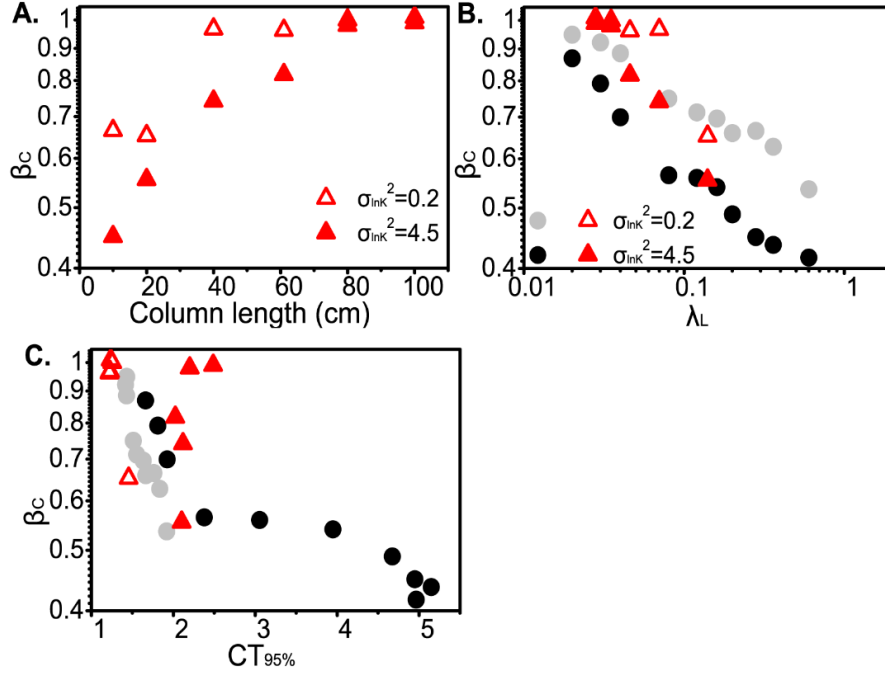
Figure 5. The βc value compares the sorption capacity between zonation columns and their corresponding Mixed columns. Large deviation of βc values from one indicates the significance of spatial heterogeneities. The βc value as a function of column length (A), relative longitudinal correlation length $\lambda_L$ (B), and connectivity (CT$_{95\%}$) (C) at two permeability variances, $\sigma^2_{lnK}$, of 4.5 and 0.2. Red color is the data obtained from column length longer than 10 cm with the same longitudinal correlation lengths of 2.8 cm. Gray and black color are data obtained from column length of 10 cm with different $\lambda_L$.

# Details of reactive transport modeling

The two-dimensional (2D) reactive transport modeling was performed to analyze the experimental data and quantify reaction kinetics at different spatial scales. The code CrunchFlow was used to calculate the concentration of species by solving the governing Advection-Dispersion-Reaction equation (Steefel and Lasaga, 1994). Species are categorized into primary or secondary species, with the former being the building blocks of the system chemistry while the secondary species can be expressed in terms of the primary species through laws of mass action (Lichtner, 1985). As an example, the reactive transport equation for Cr(VI) is written below (Miller et al., 2010):

$$\frac{\partial(C_{Cr(VI)})}{\partial t} + \frac{\rho}{\phi}\frac{\partial m}{\partial t} + \nabla(-D\nabla C_{Cr(VI)} + vC_{Cr(VI)}) = 0 \qquad (1)$$

where $C_{Cr(VI)}$ is the total concentration of all Cr(VI) - containing species (mg/m$^3$ pore volume); t is time (s); $\rho$ is the bulk density (mg/ m$^3$); $\phi$ is the porosity; m is the average adsorbed mass per unit mass of the solid phase (mg/mg); $v$ (m/s) is the flow velocity vector and can be decomposed into $v_z$ and $v_x$ in the directions parallel and transverse to the main flow; $D$ is the combined dispersion–diffusion tensor (m$^2$/s). At any particular location (grid block), their

corresponding diffusion / dispersion coefficients $D_L$ (m$^2$/s) and $D_T$ (m$^2$/s) are calculated as follows:

$$D_L = D^* + \alpha_L v_z \quad D_T = D^* + \alpha_T v \qquad (2)$$

where $\alpha_L$ and $\alpha_T$ are the longitudinal and transverse dispersivity (m), which were obtained by fitting the Br experimental data, for the zonation columns, $\alpha_T$ values were further determined by Cr(VI) breakthrough curves; D$^*$ is the effective diffusion coefficient in porous media (m$^2$/s):

$$D^* = \phi^n D_0 \qquad (3)$$

where $\phi$ is the porosity; n is the cementation factor; and D$_0$ is the molecular diffusion coefficient in water. For non-reactive species, similar equations to Eq. (1) were solved except without the reaction term $\dfrac{\rho}{\phi}\dfrac{\partial m}{\partial t}$. The thermodynamic parameters (K$_{eq}$) for aqueous speciation reactions were obtained from EQ3/6 database (Wolery et al., 1990).

In CrunchFlow, surface complexation reactions are used to represent Cr(VI) sorption process on illite (Missana et al., 2009). Surface speciation models provide a molecular description of the adsorption process based on chemical reaction equilibrium. Similar to aqueous complexation, surface complexation is considered as fast reaction and chemical thermodynamics controls the reaction (Goldberg et al., 2007). Specific surface species, equilibrium constants, mass balances, chemical reactions, and charge balances, and their molecular features are defined in these models (Dong et al., 2012; Goldberg et al., 2007; Serrano et al., 2009; Singha et al., 2013; Wen et al., 1998).

Reactive transport modeling is a useful tool for the analysis of coupled physical, chemical, and biological processes in Earth systems, and can describe the interactions of competing processes at a range of spatial and time scales. The advantages of applying the surface complexation reactions to describe adsorption in CrunchFlow include the following: it allows predictive calculations for a range of chemical conditions without adjusting the values of the model parameters, as chemical conditions are varied in space or time; it can be included efficiently in transport simulations having chemical gradients in space or time. However, there are some weaknesses. The surface complexation reactions do not have kinetic items, therefore, the model are not applicable for high flow velocity conditions. In addition, the simulation becomes slow either more reactions are involved or the scale is large. In this context, upscaling or multi-scale analysis is needed to identify strategies for multi-scale simulation.

## Products

1. Wang, L., Li, L., 2015. Illite Spatial Distribution Patterns Dictate Cr(VI) Sorption Macrocapacity and Macrokinetics. Environmental science & technology 49, 1374-1383.
2. Wang, L., Li, L. Heterogeneity controls of Cr(VI) sorption (In preparation)

3. Wang, L., and Li, L. 2014. Understanding Cr(VI) sorption in heterogeneous porous media using column experiments and reactive transport modeling. American Geophysical Union (AGU) Fall meeting, San Francisco, CA, Dec. 15-19, 2014. Abstract No. B33B-0172

4. Wang, L. and L. Li. 2013. Illite spatial distribution controls Cr(VI) adsorption capacity and kinetics. American Geophysical Union (AGU) Fall meeting, San Francisco, CA, Dec. 8- 13, 2013. Abstract No. H31D-1206

5. All data are available for public access at http://www.earthchem.org with the DOI number 10.1594/IEDA/100509.

**References:**

Chai, J.C., Onitsuk, K., Hayashi, S., 2009. Cr(VI) concentration from batch contact/tank leaching and column percolation test using fly ash with additives. Journal of Hazardous Materials 166, 67-73.

Dagan, G., 1990. Transport in Heterogeneous Porous Formations - Spatial Moments, Ergodicity, and Effective Dispersion. Water Resour Res 26, 1281-1290.

Deng, L., Shi, Z., Li, B., Yang, L.F., Luo, L., Yang, X.Z., 2014. Adsorption of Cr(VI) and Phosphate on Mg-Al Hydrotalcite Supported Kaolin Clay Prepared by Ultrasound-Assisted Coprecipitation Method Using Batch and Fixed-Bed Systems. Ind Eng Chem Res 53, 7746-7757.

Deutsch CV, J.A., 1992. GSLIB: Geostatistical Software Library and User's Guide. New York: Oxford Univ.

Dong, W.M., Tokunaga, T.K., Davis, J.A., Wan, J.M., 2012. Uranium(VI) Adsorption and Surface Complexation Modeling onto Background Sediments from the F-Area Savannah River Site. Environ. Sci. Technol. 46, 1565-1571.

Espinoza, C., Valocchi, A.J., 1997. Stochastic analysis of one-dimensional transport of kinetically adsorbing solutes in chemically heterogeneous aquifers. Water Resources Research 33, 2429-2445.

Fonseca, B., Maio, H., Quintelas, C., Teixeira, A., Tavares, T., 2009. Retention of Cr(VI) and Pb(II) on a loamy sand soil Kinetics, equilibria and breakthrough. Chemical Engineering Journal 152, 212-219.

Fox, P.M., Davis, J.A., Hay, M.B., Conrad, M.E., Campbell, K.M., Williams, K.H., Long, P.E., 2012. Rate-limited U(VI) desorption during a small-scale tracer test in a heterogeneous uranium-contaminated aquifer. Water Resour Res 48, W05512.

Gelhar, L.W., 1986. Stochastic Subsurface Hydrology from Theory to Applications. Water Resources Research 22, S135-S145.

Goldberg, S., Criscenti, L.J., Turner, D.R., Davis, J.A., Cantrell, K.J., 2007. Adsorption - Desorption processes in subsurface reactive transport modeling. Vadose Zone Journal 6, 407-435.

Jin, L., Andrews, D.M., Holmes, G.H., Lin, H., Brantley, S.L., 2011. Opening the "Black Box": Water Chemistry Reveals Hydrological Controls on Weathering in the Susquehanna Shale Hills Critical Zone Observatory. Vadose Zone Journal 10, 928-942.

Khan, A.A., Muthukrishnan, M., Guha, B.K., 2010. Sorption and transport modeling of hexavalent chromium on soil media. Journal of Hazardous Materials 174, 444-454.

Knudby, C., Carrera, J., 2005. On the relationship between indicators of geostatistical, flow and transport connectivity. Adv. Water Res. 28, 405-421.

Krishna, B.S., Murty, D.S.R., Prakash, B.S.J., 2000. Thermodynamics of chromium(VI) anionic species sorption onto surfactant-modified montmorillonite clay. Journal of Colloid and Interface Science 229, 230-236.

Landrot, G., Ajo-Franklin, J.B., Yang, L., Cabrini, S., Steefel, C.I., 2012. Measurement of accessible reactive surface area in a sandstone, with application to $CO_2$ mineralization. Chem Geol 318, 113-125.

Lichtner, P.C., 1985. Continuum model for simultaneous chemical reactions and mass transport in hydrothermal systems. Geochimica et Cosmochimica Acta 49, 779-800.

Lu, H.J., Luan, M.T., Zhang, J.L., 2010. Transport of Cr(VI) through clay liners containing activated carbon or acid-activated bentonite. Applied Clay Science 50, 99-105.

Miller, A.W., Rodriguez, D.R., Honeyman, B.D., 2010. Upscaling Sorption/Desorption Processes in Reactive Transport Models To Describe Metal/Radionuclide Transport: A Critical Review. Environmental Science & Technology 44, 7996-8007.

MirallesWilhelm, F., Gelhar, L.W., 1996. Stochastic analysis of sorption macrokinetics in heterogeneous aquifers. Water Resour Res 32, 1541-1549.

Missana, T., Alonso, U., Garcia-Gutierrez, M., 2009. Experimental study and modelling of selenite sorption onto illite and smectite clays. Journal of Colloid and Interface Science 334, 132-138.

Mohan, D., Pittman, C.U., 2006. Review: Activated carbons and low cost adsorbents for remediation of tri- and hexavalent chromium from water. Journal of Hazardous Materials 137, 762-811.

Owlad, M., Aroua, M.K., Daud, W.A.W., Baroutian, S., 2009. Removal of Hexavalent Chromium-Contaminated Water and Wastewater: A Review. Water Air Soil Poll 200, 59-77.

Peters, C.A., 2009. Accessibilities of reactive minerals in consolidated sedimentary rock: An imaging study of three sandstones. Chemical Geology 265, 198-208.

Richard, F.C., Bourg, A.C.M., 1991. Aqueous geochemistry of chromium: A review. Water Research 25, 807-816.

Serrano, S., O'Day, P.A., Vlassopoulos, D., Garcia-Gonzalez, M.T., Garrido, F., 2009. A surface complexation and ion exchange model of Pb and Cd competitive sorption on natural soils. Geochimica Et Cosmochimica Acta 73, 543-558.

Setshedi, K.Z., Bhaumik, M., Onyango, M.S., Maity, A., 2014. Breakthrough studies for Cr(VI) sorption from aqueous solution using exfoliated polypyrrole-organically modified montmorillonite clay nanocomposite. Journal of Industrial and Engineering Chemistry 20, 2208-2216.

Simunek, J., van Genuchten, M.T., 2008. Modeling nonequilibrium flow and transport processes using HYDRUS. Vadose Zone Journal 7, 782-797.

Singha, S., Sarkar, U., Luharuka, P., 2013. Functionalized granular activated carbon and surface complexation with chromates and bi-chromates in wastewater. Sci Total Environ 447, 472-487.

Smith, J.A., Sahoo, D., McLellan, H.M., Imbrigiotta, T.E., 1997. Surfactant-Enhanced Remediation of a Trichloroethene-Contaminated Aquifer. 1. Transport of Triton X-100. Environmental Science &

Technology 31, 3565-3572.

Steefel, C.I., Lasaga, A.C., 1994. A coupled model for transport of multiple chemical species and kinetic precipitation/dissolution reactions with application to reactive flow in single phase hydrothermal systems. Am. J. Sci. 294, 529-592.

Vangenuchten, M.T., Wierenga, P.J., 1976. Mass-transfer studies in sorbing porous-media .1. analytical solutions. Soil Sci. Soc. Am. J. 40, 473-480.

Vereecken, H., Vanderborght, J., Kasteel, R., Spiteller, M., Schäffer, A., Close, M., 2011. Do Lab-Derived Distribution Coefficient Values of Pesticides Match Distribution Coefficient Values Determined from Column and Field-Scale Experiments? A Critical Analysis of Relevant Literature All rights reserved. No part of this periodical may be reproduced or transmitted in any form or by any means, electronic or mechanical, including photocopying, recording, or any information storage and retrieval system, without permission in writing from the publisher. Journal of Environmental Quality 40, 879-898.

Wen, X.H., Du, Q., Tang, H.X., 1998. Surface complexation model for the heavy metal adsorption on natural sediment. Environmental Science & Technology 32, 870-875.

Wolery, T.J., Jackson, K.J., Bourcier, W.L., Bruton, C.J., Viani, B.E., Knauss, K.G., Delany, J.M., 1990. Current Status of the Eq3/6 Software Package for Geochemical Modeling. Acs Sym Ser 416, 104-116.